ELSEVIER

Catalysis Today 44 (1998) 81–92

CATALYSIS TODAY

Evaluation of relative catalytic activities of Cu(II)-exchanged L, offretite and omega gallosilicates based on Cu(II) location and adsorbate interactions determined by CW and pulsed electron spin resonance

Jong-Sung Yu*, Jeong Yeon Kim

Department of Chemistry, Hannam University, Taejon, Chungnam, 300-791, South Korea

Abstract

Three structurally related gallosilicates with L, offretite and omega zeolite structures were synthesized and cupric ion was ion-exchanged into each of these gallosilicates. The location of Cu(II) and its interaction with adsorbates in these Cu(II)-exchanged gallosilicates have been studied by electron spin resonance (ESR) and electron spin echo modulation (ESEM) spectroscopies. In fresh hydrated state, Cu(II) is located in a main channel for these materials but with different coordination numbers to water. Cu(II) is octahedrally coordinated to six water molecules in L, while Cu(II) is coordinated to three water molecules and to framework oxygens in the main channel in offretite and omega. During evacuation at increasing temperature, Cu(II) moves from the main channel towards recessed sites. Dehydration produces predominantly one Cu(II) species located in recessed sites such as hexagonal prism for L and offertite and six-ring window of a gmelinite cage for omega based on a lack of broadening of its ESR lines by added oxygen. In L and offretite gallosilicates, there is evidence for back migration of Cu(II) from a hexagonal prism into a main channel to coordinate with adsorbates. Cu(II) in L gallosilicate forms complexes with bigger molecules such as benzene, pyridine and aniline. However, no complex formation between Cu(II) and each of these bulky molecules was observed due to a distorted 12-ring entrance in offretite which makes diffusion of these bulky molecules into the main channel difficult. In omega, the back migration of Cu(II) from a gmelinite cage to a main channel was blocked and thus coordination was possible only with small molecules which can diffuse into the gmelinite cage. The L structure is likely to be the best and comparable to ZSM-5 zeolite, offretite the next and omega the least good for catalytic efficiency for exchanged transition metal ions.

Keywords: Electron spin resonance; Paramagnetic Cu(II); Catalytic activity; L; Offretite; Omega; Gallosilicates

1. Introduction

Isomorphous substitution of Al by Ga in zeolite frameworks has been of considerable interest as a route to modify the framework characteristics and geometry [1]. Gallium analogs of zeolites possess physical and chemical properties different from their aluminum analogs and thus may be potential novel materials for new catalytic applications [1,2]. The former show different gallium partitions, unit cell parameters and electronegativity and smaller T–O–

*Corresponding author. Tel.: 00 82 42 629 7446; fax: 00 82 42 629 7444; e-mail: jsyu@eve.hannam.ac.kr

0920-5861/98/$32.00
PII S0920-5861(98)00176-X

T bond angles compared to the latter [2]. Ga-loaded zeolite catalysts were found to be very active in the aromatization of light alkanes. Although the aluminosilicate moiety was reported to act as an acid-catalyst for the reaction of alkanes, gallium was suggested to play the role of dehydrogenation as well as to effect the zeolitic acidity [2](b),(c). L, offretite and omega are all structurally similar channel type molecular sieves with a 12-ring main channel. The L structure is based on channels of ϵ-cages [3], while omega is based on channels of gmelinite cages [4]. Interestingly, offretite is based on channels of both gmelinite and ϵ-cages and thus has structural characteristics of both L and omega structures [5]. L, offretite and omega are all potentially of interest as molecular sieve catalysts for moderate size molecules because of wide channels. In the present work, the location and adsorbate interactions of Cu(II) in Cu(II)-exchanged K-L, K-offretite and Na-omega gallosilicates are investigated by electron spin resonance (ESR) and pulsed ESR known as electron spin echo modulation (ESEM) to assess the catalytic potential among these three structurally related molecular sieves. These results are discussed in comparison with those for Cu(II)-doped ZSM-5 aluminosilicate zeolite as a reference point [6].

2. Experimental

2.1. Synthesis and ion exchange procedure

Gallosilicates with L, offretite and omega zeolite structures were synthesized by a modification of procedures described elsewhere [7–9]. The powder X-ray diffraction (XRD) patterns of as-synthesized gallosilicate materials are shown in Fig. 1 and agree with literature data [3–5]. The chemical compositions of as-synthesized materials determined by an inductively coupled plasma spectrometer in combination with atomic absorption analysis and the BET surface areas determined from nitrogen adsorption are summarized in Table 1. As-synthesized offretite and omega gallosilicate were calcined in flowing O_2 at

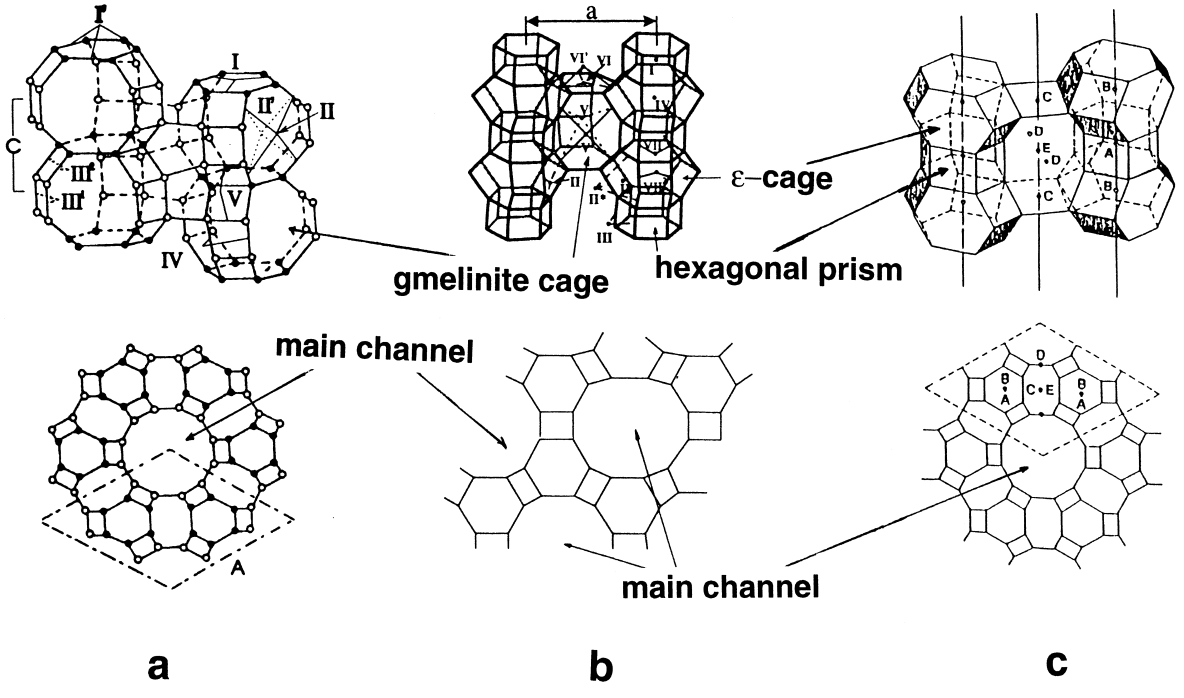

Fig. 1. Schematic representation viewed approximately perpendicular (upper) and parallel (lower) to the *c*-axis of (a) omega, (b) offretite, and (c) L structures. *T* atoms (Si, Al and Ga atoms) are represented by the corners of the rings and oxygens are represented by the center of each line. The cation sites are indicated by Roman numerals and capital letters.

Table 1
Chemical compositions and BET surface areas of gallosilicate molecular sieves prepared in this work

Sample	Chemical composition per unit cell[a]	BET surface area[b] ($m^2\ g^{-1}$)
L	$K_{10.0}Ga_{10.0}Si_{26.0}O_{72.0}\cdot 49.1H_2O$	464
Offretite	$TMA_{0.9}Na_{1.2}K_{3.1}$ $Ga_{5.2}Si_{12.8}O_{36.0}\cdot 9.9H_2O$	444
Omega	$TMA_{2.0}Na_{8.0}Ga_{10.0}$ $Si_{26.0}O_{72.0}\cdot 16.8H_2O$	850

[a]Fully hydrated.
[b]BET surface areas calculated from nitrogen adsorption data for the sample calcined under the flowing O_2 at 773 K.

550°C for 10 and 1 h to remove occluded tetramethylammonium (TMA) ion template to give the H, Na, K-form of offretite and the H, Na form of omega, respectively. The calcined offretite and an as-synthesized K-L were then washed four times with 0.1 M potassium acetate at 70°C to ensure the K-exchanged form according to the procedure in previous work [10]. The calcined omega samples were refluxed four times in 0.1 M $NaNO_3$ for 12 h at 70°C to ensure complete Na exchange. Each of these gallosilicate samples was further partially exchanged at room temperature for 12 h by dropwise addition of 10 mM copper(II) nitrate (Alfa) according to the procedure described in earlier work [11]. Copper exchanges were 0.19–0.30% by weight of the gallosilicate. All the characteristic XRD peaks of each of these gallosilicates remain intact after Cu(II) ion exchange and thermal treatment up to 430°C.

2.2. Sample treatment

The samples were loaded directly into Suprasil quartz ESR tubes (2 mm i.d. by 3 mm o.d.) which could be connected to a vacuum and gas handling line. Dehydration for the gallosilicate was carried out by first evacuating the sample at room temperature followed by heating to 200°C over an 8 h period in a static reactor under vacuum. In general, gallosilicate is known to have lower thermal stability compared to the corresponding aluminosilicate zeolite [1]. Thus no evacuation was usually made at temperatures higher than 250°C in this work. Following evacuation the sample was exposed to 200–400 Torr of high-purity dry oxygen for 5–10 h at 410°C in order to oxidize any copper species that might have been reduced during the heating period. Finally, the oxygen was pumped off at room temperature under a 10^{-5} Torr vacuum. This heat treated sample by oxygen is termed as a dehydrated sample.

After dehydration, adsorbates were admitted at room temperature to the sample tubes and left to equilibrate. Deuterated adsorbates D_2O, CD_3OH, CH_3OD, CH_3CH_2OD, $CH_3CH_2CH_2OD$, ND_3, C_6D_6, C_5ND_5 and C_2D_4 and other isotope enriched adsorbates ^{13}CO and $^{15}NH_3$ were obtained from Aldrich, Stohler Isotope Chemicals and Cambridge Isotope Laboratories and used after repeated freeze-pump-thaw cycles.

2.3. Instrumental measurements

Thermogravimetric analysis (TGA) and differential thermal analysis (DTA) were performed on a Dupont 950 thermogravimetric analyzer and a Rigaku differential thermal analyzer, respectively. Chemical analysis was performed by a Jarrel-Ash Polyscan 61E inductively coupled plasma spectrometer in combination with a Perkin-Elmer 5000 atomic absorption spectrometer. The nitrogen BET surface areas were measured on a Micromeritics ASAP 2000 analyzer. ESR spectra were measured at 77 K and at room temperature on a Bruker ESP 300 and a modified Varian E-4 spectrometer interfaced to a Tracor Northern TN-1710 signal averager. ESEM spectra were recorded with a Bruker ESP 380 pulsed ESR spectrometer. Three-pulse echoes were measured by using a 90°-*t*- 90°-*T*-90° pulse sequence with the echo measured as a function of *T*. In a typical ESEM study, the deuterium modulation from a deuterated adsorbate is analyzed to determine its coordination to Cu(II). Both the theory and methods for ESEM measurements and simulation of the data are described in detail elsewhere [12,13].

3. Results and discussion

3.1. Crystal structures of omega, offretite and L

Schematic structures of omega, offretite and L are shown in Fig. 2. The crystal structure of omega consists of gmelinite cages which are linked in columns

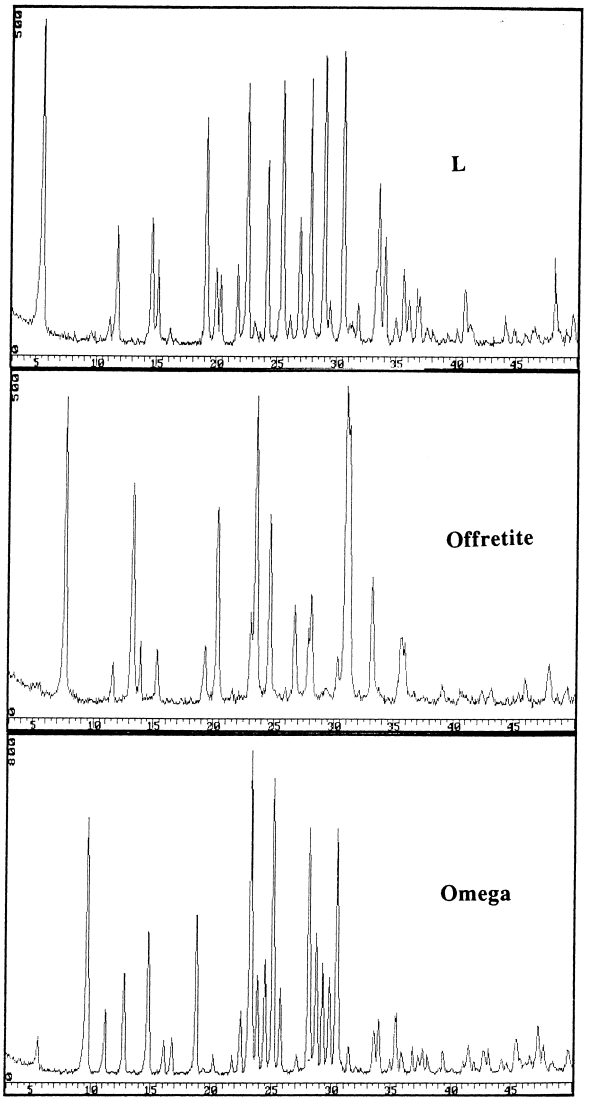

Fig. 2. X-ray diffraction (XRD) patterns of as-synthesized L, offretite and omega gallosilicates.

parallel to the *c*-axis as illustrated in Fig. 2(a) [4,9]. The unit cell contains two gmelinite cages shifted by *c*/2. The columns of 14-hedra gmelinite cages are linked laterally by oxygen bridges through the four-rings into a hexagonal array to create and surround wide channels of 12-membered rings also parallel to the *c*-axis. These wide channels, usually called main channels, have an average free aperture of ~0.74 nm. There are two other smaller channels parallel to the *c*-axis. The first one is the channel of six-membered rings through gmelinite cages. The other one is formed between two cross-linked rows of gmelinite cages and is surrounded by eight-membered rings. There is also one two-dimensional channel system in the plane perpendicular to the *c*-axis formed through distorted eight-membered rings of 14-hedra gmelinite cages. Interestingly this channel system is not accessible to the main 12-ring channel, and does not connect in the *c*-direction except through small six-rings. Access to this channel system is available only at the surface. The walls of main channels consist of four-membered rings bordering the gmelinite cages and five-membered rings bordering the eight-ring channels parallel to the *c*-axis.

The crystal structure of L is based on the 11-hedra ϵ-cages as shown in Fig. 2(c) [3,7]. The ϵ-cages are linked through their nearly planar six-membered rings, forming hexagonal prisms with the planes of the six-membered rings normal to the *c*-axis. Thus L zeolite consists of a series of columns along the *c*-axis where ϵ-cages and hexagonal prism units alternate. The columns are linked to each other laterally by oxygen bridges to produce wide main channels of twelve-membered rings with free diameters of 0.71–0.78 nm parallel to the *c*-axis.

Interestingly the crystal structure of offretite has characteristics of both the omega and L structures since it is based on two types of columns of 14-hedra gmelinite cages and of 11-hedra ϵ-cages alternating with hexagonal prisms seen in the omega and L structures, respectively, as shown in Fig. 2(b) [5,8]. These two types of column in the direction of the *c*-axis alternate and are cross-linked so as to create wide main channels of 12-membered rings with free diameters of ~0.67 nm also parallel to the *c*-axis.

There are several different types of probable cation sites shown in the each of crystal structures. These cations sites are indicated by Roman numerals for omega and offretite structures and by capital letters for L.

Fig. 3 shows the electron diffraction pattern and lattice fringe image from CuK-offretite gallosilicate. The electron diffraction pattern of CuK-offretite gallosilicate shows no streak, indicating that stacking faults are absent [14] (Fig. 3(a)). This is further supported in the lattice fringe images as shown in Fig. 3(b) which shows no irregular array of stacking.

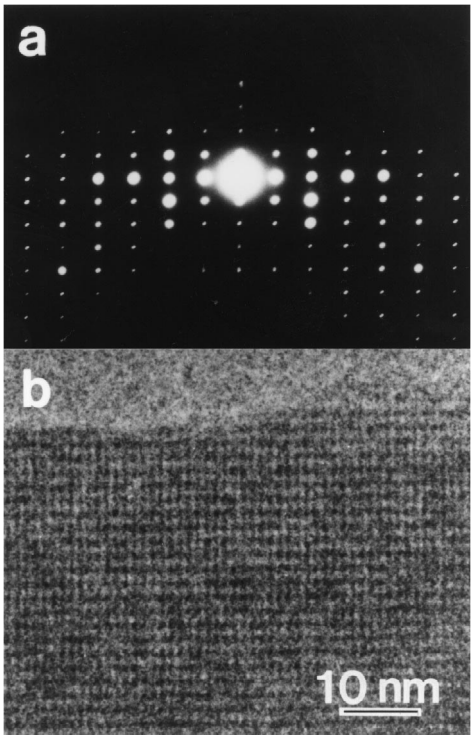

Fig. 3. (a) Electron diffraction pattern and (b) lattice fringe image of CuK-offretite gallosilicate.

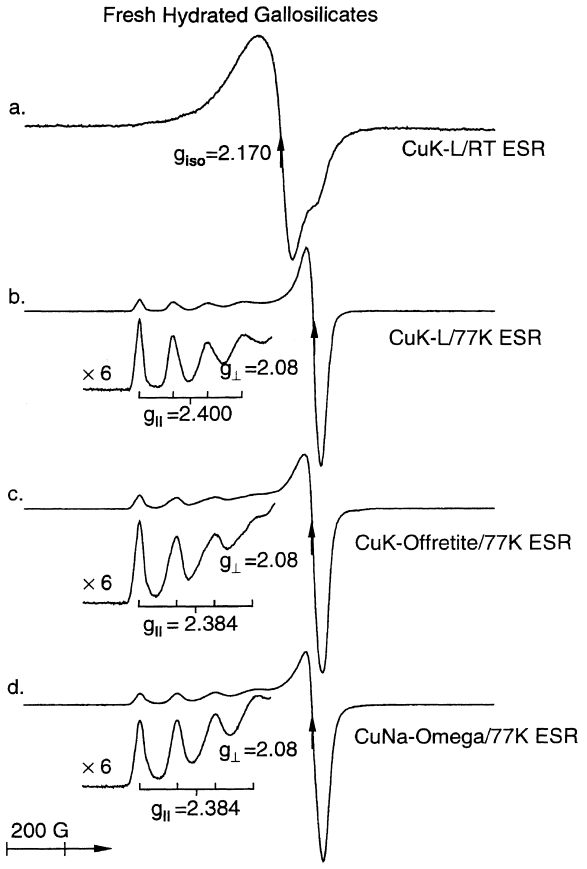

Fig. 4. ESR spectra of fresh hydrated sample of (a) CuK-L gallosilicate recorded at room tempearture and (b) CuK-L gallosilicate at 77 K, (c) CuK-offretite gallosilicate at 77 K, and (d) CuNa-omega gallosilicate at 77 K.

3.2. Adsorbate interactions

The probable Cu(II) location and adsorbate coordination can be determined on the basis of the ESR and ESE parameters for Cu(II) species in connection with the characteristics of the framework structure of the host materials. The Cu(II) spin Hamiltonian parameters usually provide some guide to the overall coordination symmetry of the metal ion site based on extensive studies of known Cu(II) crystalline compounds. Together with the number of adsorbed molecules determined by ESEM and a comparison with known Cu(II) locations in zeolites, the Cu(II) ESR parameters provide information about the coordination and location of Cu(II) ions exchanged into gallosilicate molecular sieves. L, offretite and omega structures all have 12-ring main channels in common. Interestingly, however, their coordination capacities for adsorbates to Cu(II) ion-exchanged into each structure are rather different.

Fig. 4 shows the ESR spectra at room temperature and 77 K of fresh, hydrated CuK-L, CuK-offretite and CuNa-omega gallosilicates before dehydration. The fresh, hydrated sample measured at 77 K before evacuation produces an anisotropic ESR signal characteristic of an axial powder spectrum of Cu(II) with the ESR parameters of $g_{\|}$=2.400 and $A_{\|}$= 134×10^{-4} cm^{-1} as shown in Fig. 4(b). The hyperfine lines of the perpendicular component are not resolved. A value of $g_{\perp}$=2.08 is estimated for the perpendicular component of the g tensor. The ESR spectrum measured at room temperature, however, shows an almost isotropic signal at g_{iso}=2.17 as shown in Fig. 4(a).

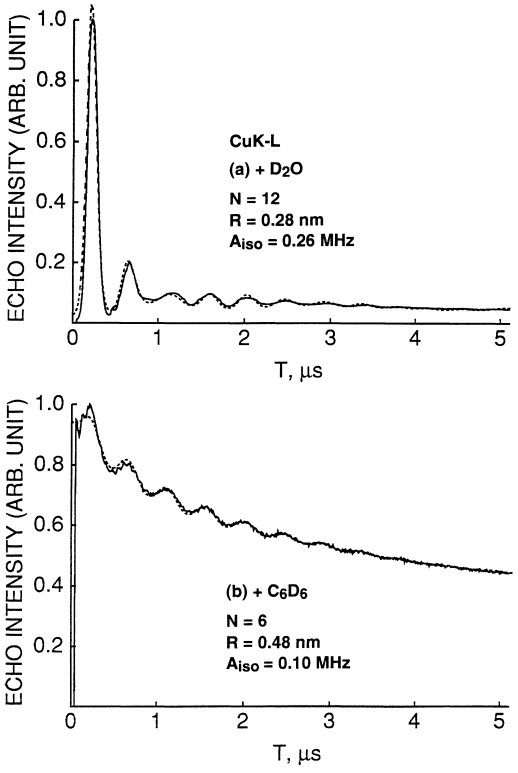

Fig. 5. Experimental (———) and simulated (- - - - -) three-pulse ESEM spectra recorded at 4.5 K of dehydrated CuK-L gallosilicate with adsorbed (a) D_2O, and (b) C_6D_6.

One Cu(II) species is predominantly observed with the ESR parameters of $g_{\|}$=2.384, $A_{\|}$=145×10^{-4}–147×10^{-4} cm^{-1} and $g_{\perp}$=2.08 for 77 K ESR of hydrated CuK-offretite and CuNa-omega. When measured at room temperature, a similar anisotropic ESR signal is also observed unlike in CuK-L. An isotropic ESR signal at room temperature for CuK-L is indicative of a rotating species. Analysis of the three-pulse ESEM spectrum (Fig. 5(a)) of dehydrated gallosilicate which has been rehydrated with D_2O and which exhibited an identical ESR spectrum to the fresh CuK-L indicates 12 nearest deuteriums corresponding to a water solvation number of 6 around Cu(II), i.e., $[Cu(H_2O)_6]^{2+}$. At 77 K this $[Cu(H_2O)_6]^{2+}$ complex becomes immobilized and gives rise to an asymmetric spectrum as shown in Fig. 4(b). The L structure has 12-membered ring main channels whose diameter is about 0.71–0.78 nm, large enough to accommodate a hexaaquo complex [7]. The anisotropic room temperature ESR spectra observed in the hydrated Cu(II)-offretite and Cu(II)-omega gallosilicate suggest that the Cu(II) species is not octahedrally hydrated, and is rather anchored to zeolite lattice by coordination to zeolitic oxygens. In this way the Cu(II) ions would become rigidly bound to the zeolite framework with a resultant loss of mobility leading to the observed g factor ansiotropy in the ESR spectrum. When Cu(II) loses water molecules during evacuation, Cu(II) moves towards channel wall or recessed sites so as to maintain coordination sphere by coordinating to framework oxygens. Tables 2 and 3 summarize the ESR parameters and ESEM parameters of Cu(II) in CuK-L, CuK-offretite and CuNa-omega gallosilicates after various sample treatments. Analyses of the three-pulse ESEM spectra (figures not shown) of dehydrated K-offretite and Na-omega gallosilicates rehydrated with D_2O indicate a water solvation number of 3 around Cu(II) for both structures. This also indicates that the Cu(II) species is not octahedrally hydrated, and supports the ESR data.

Upon adsorption of benzene, a new signal is observed with $g_{\|}$=2.350, $A_{\|}$=140×10^{-4} cm^{-1} and $g_{\perp}$=2.07 (figure not shown). The deuterium modulation observed in the three-pulse ESEM spectrum of dehydrated CuK-L gallosilicate with adsorbed C_6D_6 is best simulated by six interacting deuterium nuclei at a distance of 0.48 nm with A_{iso}=0.10 MHz (Fig. 5(b)). This indicates one directly interacting benzene molecule via π-bonding.

Fig. 6 shows the ESR spectra at 77 K observed after dehydration and after adsorption of alcohols following dehydration of CuK-L samples. Dehydration produces predominantly one Cu(II) species. About 100 Torr dry oxygen was added into the dehydrated sample to assess the Cu(II) site locations. Cu(II) is suggested to be located in a site recessed from a main channel such as a hexagonal prism based on a lack of broadening of its ESR lines by added oxygen. Adsorption of methanol produces an ESR spectrum with $g_{\|}$=2.381, $A_{\|}$=132×10^{-4} cm^{-1} and $g_{\perp}$=2.09 as shown in Fig. 6(b). Similar ESR spectra are observed upon adsorption of ethanol and propanol (Fig. 6(c) and (d)). Analyses of three-pulse ESEM spectra indicate that Cu(II) is coordinated to two molecules of methanol, ethanol and propanol, respectively (see Table 3). This indicates that upon adsorption of alcohols, Cu(II) migrates back from a recessed hexagonal prism site

Table 2
ESR parameters at 77 K of Cu(II) in CuK-L, CuK-offretite and CuNa-omega gallosilicates observed after various sample treatments

Treatment	L			Offretite			Omega		
	$g_{\|}$[a]	$A_{\|}$[b]	$g_{\perp}$[c]	$g_{\|}$[a]	$A_{\|}$[b]	$g_{\perp}$[c]	$g_{\|}$[a]	$A_{\|}$[b]	$g_{\perp}$[c]
Fresh/RT ESR[d]	2.17[e]								
Fresh	2.400	134	2.08	2.384	146	2.08	2.384	147	2.08
Dehydrated	2.338	153	2.07	2.335	156	2.05	2.332	169	2.07
$+H_2O$	2.399	134	2.08	2.384	145	2.08	2.385	147	2.08
$+CH_3OH$	2.381	132	2.09	2.384	135	2.08	2.372	142	2.08
$+CH_3CH_2OH$	2.381	128	2.09	2.382	135	2.08	2.373	135	2.08
$+CH_2CH_3CH_2OH$	2.380	131	2.08	2.386	132	2.08	NI	NI	NI
$+C_2H_4$	2.344	148	0.07	2.337	157	2.05	2.381	146	2.08
$+NH_3$	2.254	175	2.05	2.004	90	2.20	2.242	193	2.06
$+C_6C_6$	2.350	140	2.07	NI	NI	NI	NI	NI	NI
+Pyridine	2.255	187	2.06	NI	NI	NI	NI	NI	NI
+Aniline	2.270	145	2.06	NI	NI	NI	NI	NI	NI

NI – no interaction.
[a]Estimated uncertainty is ± 0.007.
[b]The unit of $A_{\|}$ is 1×10^{-4} cm^{-1} and the estimated uncertainty is $\pm7\times10^{-4}$ cm^{-1}.
[c]Estimated uncertainty is ± 0.01.
[d]ESR measured at room temperature.
[e]g_{iso} value.

Table 3
ESEM parameters[a] for Cu(II) with various deuterated adsorbates compared among CuK-L, CuK-offretite and CuNa-omega gallosilicates

Adsorbates	L			Offretite			Omega		
	N	R (nm)	A_{iso} (MHz)	N	R (nm)	A_{iso} (MHz)	N	R (nm)	A_{iso} (MHz)
$+D_2O$	12	0.28	0.26	6	0.27	0.21	6	0.29	0.27
$+CD_3OH$	6	0.38	0.13	6	0.37	0.18	6	0.40	0.10
$+CH_3OD$	2	0.28	0.25	2	0.27	0.28	2	0.29	0.29
$+CH_3CH_2OD$	2	0.28	0.28	2	0.29	0.28	1	0.30	0.29
$+CH_3CH_2CH_2OD$	2	0.29	0.28	2	0.30	0.29	NI	NI	NI
$+C_2D_4$	4	0.40	0.09	4	0.35	0.12	4	0.48	0.15
$+C_6D_6$	6	0.48	0.10	NI	NI	NI	NI	NI	NI
$+C_5D_5N$	8	0.30	0.70[b]	NI	NI	NI	NI	NI	NI
	8	0.48	0.41[b]						

NI – no interaction.
[a]N is the number of deuterium nuclei, R is the Cu(II) to D distance, and A_{iso} is the isotropic hyperfine coupling. Estimated uncertainty is ± 0.01 nm in R and $\pm 10\%$ in A_{iso}.
[b] Two-shell model for simulation of deuterium modulation with deuterated pyridine, C_5D_5N.

towards a main channel to form a Cu(II)–alcohol complex in the main channel.

Fig. 7 shows the ESR spectra at 77 K observed after adsorption of different adsorbates on dehydrated CuNa-omega gallosilicate. Fig. 7(a) shows predominantly one Cu(II) species, denoted as species Dh after dehydration. Species Dh is also assigned to a site recessed from a main channel such as a six-ring window in a gmelinite cage based on a lack of broadening of its ESR lines by added oxygen. Rehydration of the dehydrated sample by exposure to the vapor pressure of water at room temperature results in the ESR spectrum shown in Fig. 7(b). A new species with $g_{\|}=2.385$, $A_{\|}=147\times10^{-4}$ found in freshly hydrated

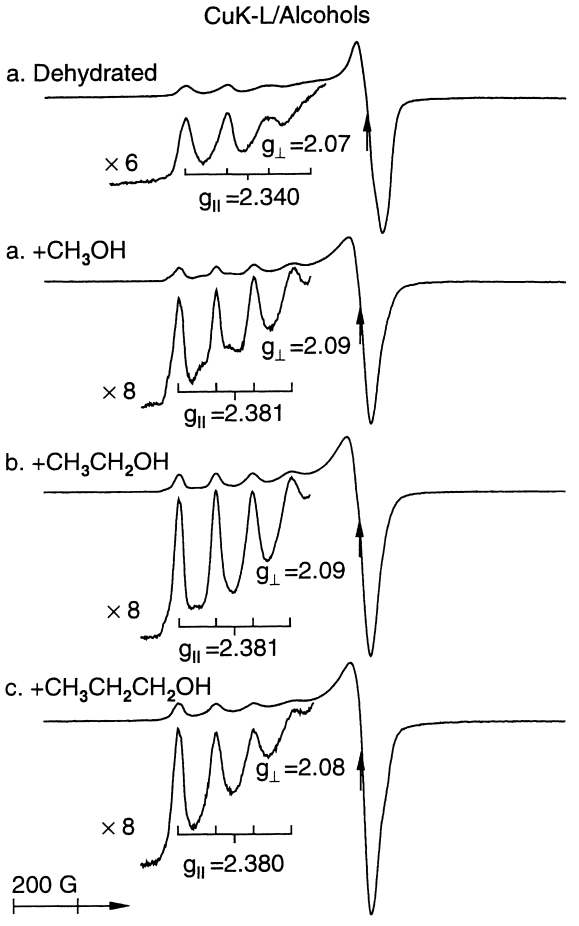

Fig. 6. ESR spectra at 77 K of CuK-L gallosilicate (a) after dehydration, (b) after dehydration as in (a) and after adsoption of methanol, (c) after dehydration as in (a) and after adsoption of ethanol, and (d) after dehydration as in (a) and after adsoption of propanol.

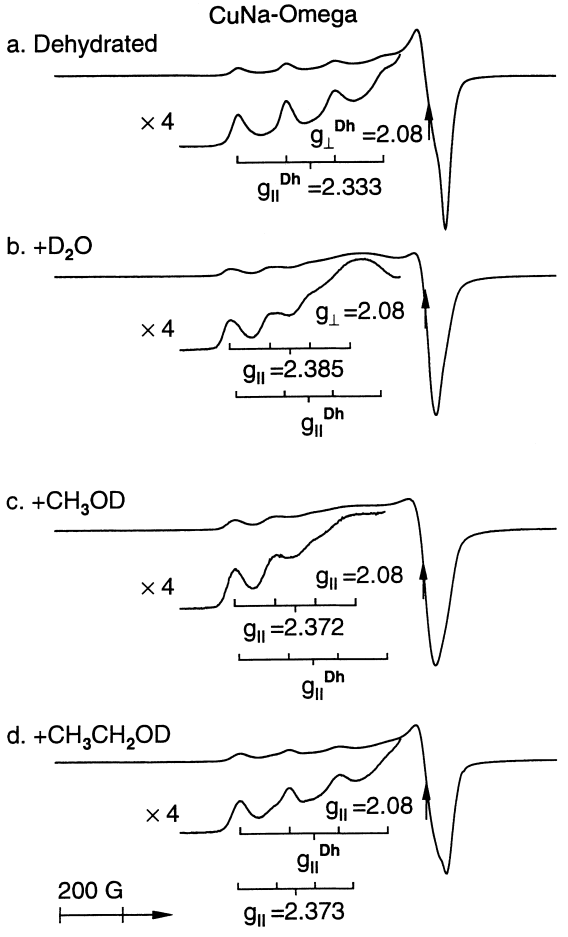

Fig. 7. ESR spectra at 77 K of CuNa-omega gallosilicate measured (a) after dehydration, (b) after dehydration as in (a) and absorption of D_2O at room temperature, (c) after dehydration as in (a) and adsorption of CH_3OD at room temperature and heating at 110°C for 10 h, and (d) after dehydration as in (a) and adsorption of CH_3CH_2OD at room temperature and heating at 110°C for 10 h.

samples is slowly regenerated from species Dh. However, some of species Dh is still observed and overlaps with the new species suggesting that not all species Dh can be rehydrated.

Adsorption of methanol causes very little change in ESR spectrum over a few hours. After several days, the new Cu(II) species is clearly observed with $g_{\|}$=2.372, $A_{\|}$=142×10^{-4} cm^{-1} and $g_{\perp}$=2.08 overlapped with species Dh. When a sealed ESR sample tube with added methanol vapor was heated in an oven set at the temperature of 110°C for 10 h, the intensity of a new Cu(II) species increases as shown in Fig. 7(c). Similar but slower changes in the ESR spectra are observed upon adsorption of ethanol. Fig. 7(d) shows the ESR spectrum measured at 77 K after heating a sealed tube with added ethanol for 10 h. The new Cu(II) species is observed only weakly on the shoulder of species Dh. Similar to the results for water vapor adsorption, not all species Dh interact with alcohol to form a new Cu(II) species. Upon propanol adsorption, very little change in ESR spectrum was observed even after heating at 110°C for several days, indicating no interaction between Cu(II) and propanol in omega gallosilicate.

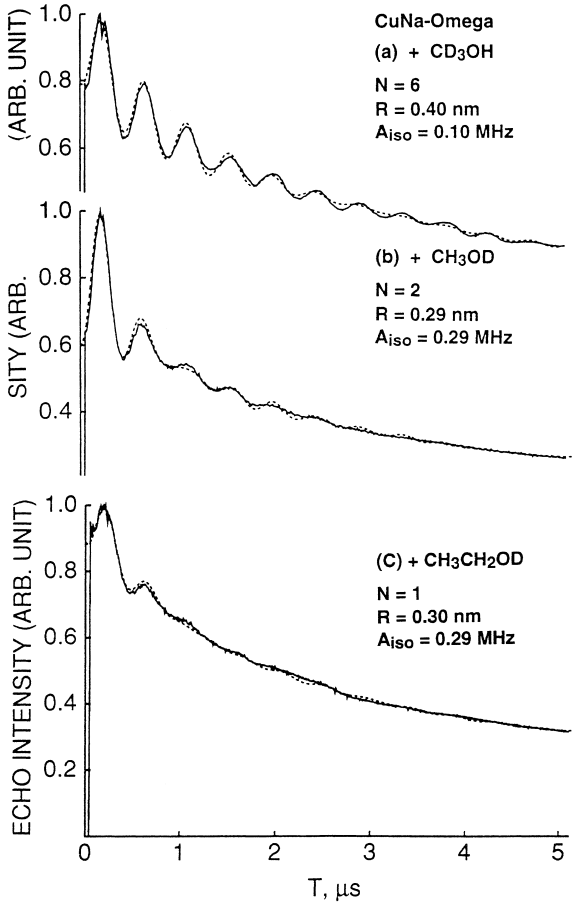

Fig. 8. Experimental (———) and simulated (- - - - -) three-pulse ESEM spectra recorded at 4.5 K of dehydrated CuNa-omega gallosilicate with adsorbed (a) CD_3OH, (b) CH_3OD, and (c) CH_3CH_2OD.

The three-pulse ESEM spectra of dehydrated CuNa-omega gallosilicate with adsorbed CD_3OH, CH_3OD and CH_3CH_2OD are shown in Fig. 8. The simulation for CD_3OH indicates interaction with six deuterium nuclei, i.e., two molecules of methanol, with a Cu(II)–D distance of 0.40 nm (Fig. 8(a)). The simulation for CH_3OD indicates interaction with two deuterium nuclei, i.e., two molecules of methanol, with a Cu(II)–D distance of 0.29 nm (Fig. 8(b)). Both results are self-consistent and indicate that Cu(II) directly coordinates to two molecules of methanol through the hydroxyl oxygen. The simulation of relatively shallow deuterium modulation for CH_3CH_2OD adsorption indicates interaction with one deuterium nucleus with a Cu(II)–D distance of 0.30 nm as shown in Fig. 8(c). This result indicates that only one ethanol molecule is coordinated to Cu(II) unlike for methanol adsorption. This is consistent with weak development of a new Cu(II) species upon ethanol adsorption (see Fig. 7(d)).

Adsorption of methanol on dehydrated CuK-offretite produces a single species in the ESR spectrum and results in a complex involving two molecules of methanol from an analysis of the ESEM spectrum (see Table 3). Adsorption of ethanol and propanol also gives very similar ESR parameters as adsorption of methanol (see Table 2). The ESEM spectra also indicate that Cu(II) is coordinated to two molecules of ethanol and propanol, respectively (Fig. 10(b)).

Interestingly, however, the times for complex formation between Cu(II) and alcohols are quite different for these three different structurally related gallosilicates. It did not change much for L gallosilicate (all about 10–30 min for methanol to propanol), but increased with increasing chain length of the alcohols in offretite gallosilicate (10–30 min for methanol or ethanol over 20 h for propanol) [7,8]. It took much more time in the omega structure. Cu(II) does not form a complex with propanol or larger adsorbates in omega. Thus in omega the back migration from a gmelinite cage to a main channel seems to be blocked as shown by very slow changes in ESR spectra and differing coordination numbers for methanol, ethanol and propanol to Cu(II) when alcohols are adsorbed. Migration from a gmelinite cage to a main channel through a distorted five-ring in a dehydrated CuNa-omega is likely to be difficult upon adsorption of adsorbates.

The ESR spectrum of dehydrated CuK-L gallosilicate measured after pyridine adsorption is shown in Fig. 9(a). A new cupric ion species due to complex formation with pyridine is observed with at least nine hyperfine lines centered at g=2.055 and split by 15×10^{-4} cm^{-1} as shown in the expanded second-derivative spectrum. Fig. 9(b) shows the ESR spectra after adsorption of NH_3 onto dehydrated CuK-L gallosilicates. CuK-L with adsorbed NH_3 (^{14}N has a nuclear spin of 1) shows nine ^{14}N hyperfine lines centered at g=2.052 and split by 13×10^{-4} cm^{-1}. With adsorbed $^{15}NH_3$ (^{15}N has a nuclear spin of 1/2), the ESR spectrum shows five ^{15}N hyperfine lines centered at g=2.054 and split by 18×10^{-4} cm^{-1} which are shown

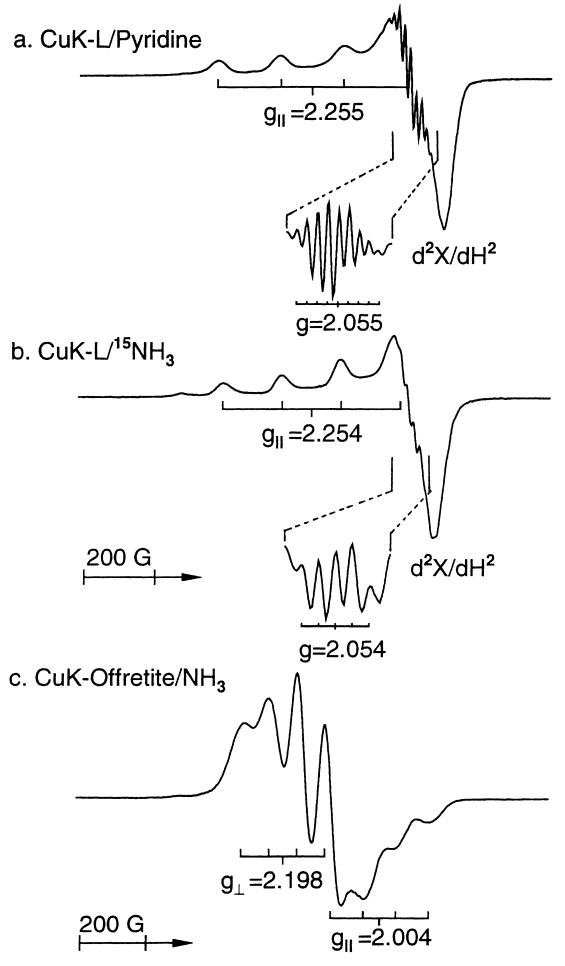

Fig. 9. ESR spectra at 77 K of: (a) dehydrated CuK-L gallosilicate equilibrated with pyridine containing ^{14}N, (b) dehydrated CuK-L gallosilicate after adsorption of 50 Torr $^{15}NH_3$, and (c) dehydrated CuK-offretite gallosilicate after adsorption of 40 Torr of NH_3 at room temperature.

in the expanded second-derivative spectrum in the bottom of Fig. 9(b). This indicates that Cu(II) coordinates to four molecules of pyridine and ammonia, respectively. Similar *N* superhyperfine lines are observed in Cu(II)-omega gallosilicate upon adsorption of ammonia, thus allowing independent determination of the coordination numbers of four interacting ammonium molecules. Tetracoordinated cupric complexes such as CuX_4(X=Cl, NH_3, etc.) generally prefer a square-planar configuration [15]. Thus, in this case the Cu(II) species is suggested to be located in the center of the 12-ring main channel, coordinating to four ammonias in a square-planar geometry. The L structure also has a bigger cage-like space inside channel with a maximum internal diameter of 1.3 nm which can enable the maximum coordination. Cu(II) is likely to be located there for the formation of a tetrapyridine complex, $[Cu(C_5H_5N)_4]^{2+}$ in a square-planar geometry.

Fig. 9(c) shows the ESR spectrum at 77 K after adsorption of ammonia gas upon a dehydrated CuK-offretite. The ESR spectrum shows a drastic change with the formation of a new Cu(II) species with the reverse ESR parameters of $g_{\|}=2.004$, $A_{\|}=90\times 10^{-4}\,cm^{-1}$, $g_{\perp}=2.198$, and $A_{\perp}=86\times 10^{-4}\,cm^{-1}$ which are quite different from those in L and omega gallosilicates. Identical ESR spectra are observed upon adsorption of $^{14}NH_3$ and $^{15}NH_3$. No resolved nitrogen hyperfine lines are observed in this sample. Nitrogen hyperfine interactions may be hidden by much stronger stereospecific effect of anisotropic Cu(II) *g* tensor. The parameter $g_{\|}$ being less than $g_{\perp}$ for Cu(II) occurs when the unpaired spin has a $|3z^2-r^2>$ orbital as the dominant part of the ground state wave function [16]. Herman [17] reported the Cu(II) ESR spectra with the reversed *g* values upon ammonia adsorption and suggested it to be the trigonal bipyramidal complex of Cu(II) with two ammonias in axial positions and three oxygens in the planar six-ring window. The analysis of the three-pulse ESEM spectrum of CuK-offretite with adsorbed ND_3 (Fig. 10(a)) indicates two ammonia molecules directly coordinated to Cu(II). Thus it is tentatively suggested that Cu(II) forms a diammonia complex with trigonal bipyramidal structure with two ammonias in axial positions, one in the main channel and the other in an ϵ-cage and three framework oxygens in the six-ring window of the ϵ-cage.

However, upon adsorption of benzene, pyridine and aniline on dehydrated offretite and omega gallosilicate at room temperature, no change of the ESR spectrum is observed, indicating no interaction between Cu(II) and these bulky adsorbates (see Table 2).

Anderson and Kevan [6] studied the Cu(II) adsorbate interactions in Cu(II)-doped ZSM-5 aluminosilicate zeolite by ESR techniques. Cu(II) was found to be octahedrally coordinated to six water molecules at the interaction between two zeolitic channels. They also reported that adsorption of adsorbate molecules such as water, ammonia, alcohols, benzene and

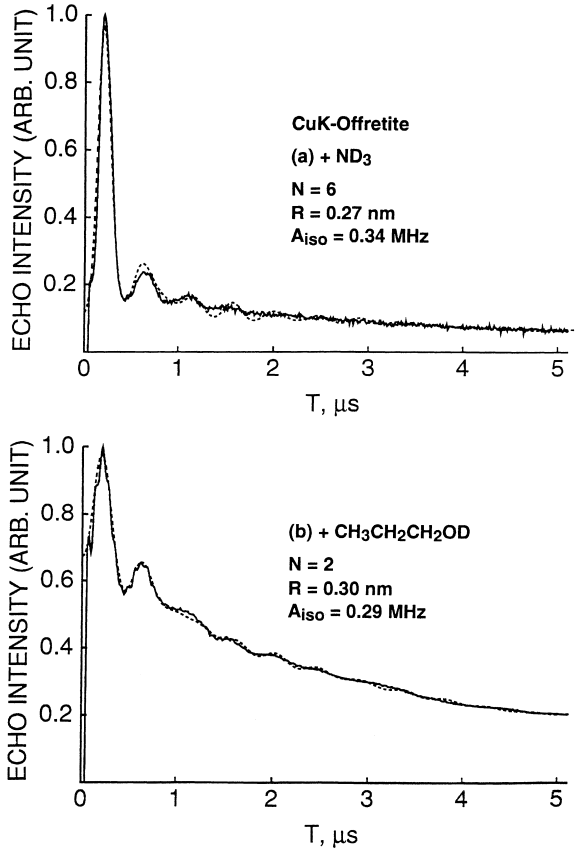

Fig. 10. Experimental (———) and simulated (- - - - -) three-pulse ESEM spectra recorded at 4.5 K of dehydrated CuK-offretite gallosilicate with adsorbed (a) ND_3, and (b) $CH_3CH_2CH_2OD$.

pyridine caused the rapid migration of the Cu(II) from recessed sites in a dehydrated state into cation position in the main channels. These results are very comparable to those for L gallosilicate.

4. Conclusions

L, offretite and omega gallosilicates all have 12-ring main channels in common. Interestingly, however, their coordination capacities for adsorbates to Cu(II) ion-exchanged into each structure are rather different. Cu(II) forms hexaquo species only in the L structure and coordinates to only three water molecules in omega and offretite in hydrated state. L and offretite structures show about the same adsorbate interactions for small molecules such as alcohols, ethylene and NH_3. However the time for complex formation between Cu(II) and alcohols was similar on L gallosilicate, but increased with increasing chain length of the alcohols in offretite gallosilicate and required much longer times in the omega structure. Cu(II) does not form a complex with propanol or larger adsorbates in omega.

Cu(II) in L gallosilicate also forms complexes with bigger molecules such as benzene, pyridine and aniline. However, no complex formation between Cu(II) and each of these bulky molecules was observed by ESR and ESEM spectroscopies in offretite. This may be ascribed to a distorted 12-ring entrance which makes diffusion of these bulky molecules into the main channel difficult. In omega, Cu(II) migration was blocked and thus coordination was possible only with small molecules which can diffuse into the gmelinite cage. The L structure has a wide channel and a bigger cage-like space inside the channel with a maximum internal diameter of 1.3 nm which can enable the maximum coordination with small and medium size molecules. Thus the L structure appears to be the best and comparable to ZSM-5 zeolite, offretite the next and omega the least good for catalytic accessibility for exchanged transition metal ions.

Acknowledgements

This research was supported by Hannam University. The authors are grateful to Prof. Larry Kevan at University of Houston for ESEM measurements. We also thank Prof. Jeong Yong Lee at KAIST for ED pattern and lattice fringe image pictures and Dr. S.B. Hong at KIST in Korea for sample preparation.

References

[1] J.M. Newsam, D.E.W. Vaughan, Stud. Surf. Sci. Catal. 28 (1986) 457.
[2] (a) R.M. Barrer, Hydrothermal Chemistry of Zeolites, Academic Press, London, 1982, p. 251; (b) J.M. Thomas, X.S. Liu, J. Phys. Chem. 90 (1986) 4843; (c) P. Mariaudeau, G. Sapaly, G. Wicker, C. Naccache, Catal. Lett. 27 (1994) 143.
[3] J.M. Newsam, Mat. Res. Bull. 21 (1986) 661.
[4] E. Ponthieu, P. Grange, J.F. Joly, F. Raatz, Zeolites 12 (1992) 395.

[5] J.M. Bennett, J.A. Gard, Nature 214 (1967) 1005.
[6] M.W. Anderson, L. Kevan, J. Phys. Chem. 91 (1987) 4174.
[7] J.-S. Yu, S.J. Kim, S.B. Hong, L. Kevan, J. Chem. Soc., Faraday Trans. 92 (1996) 855.
[8] J.-S. Yu, J.W. Ryoo, S.J. Kim, S.B. Hong, L. Kevan, J. Phys. Chem. 100 (1996) 12624.
[9] R.H. Jarman, A.J. Jacobson, M.T. Melchior, J. Phys. Chem. 88 (1984) 5748.
[10] J.-S. Yu, L. Kevan, J. Phys. Chem. 95 (1991) 3262.
[11] J.-S. Yu, J.-M. Comets, L. Kevan, J. Phys. Chem. 97 (1993) 11047.
[12] L. Kevan, in: L. Kevan, M.K. Bowman (Eds.), Modern Pulsed and Continuous-Wave Electron Spin Resonance, Chapter 5, Wiley/Interscience, New York, 1990.
[13] A. Benetis, A. Westerling, J. Magn. Reson. 86 (1990) 97.
[14] J.A. Gard, J.M. Tait, Adv. Chem. Ser. 101 (1971) 230.
[15] K.F. Purcell, J.C. Kolts, Inorganic Chemistry, Chapter 9, Saunders, Philadelphia, 1977.
[16] A. Abragam, B. Bleaney, Electron Paramagnetic Resonance of Transition Ions, Clarendon Press, Oxford, 1970, p. 456.
[17] R.G. Herman, Inorg. Chem. 18 (1979) 995.